Light Stimulates a Transducin-Independent Increase of Cytoplasmic Ca^{2+} and Suppression of Current in Cones from the Zebrafish Mutant *nof*

Susan E. Brockerhoff,[1] Fred Rieke,[2] Hugh R. Matthews,[3] Michael R. Taylor,[1] Breandan Kennedy,[1] Irina Ankoudinova,[1] Gregory A. Niemi,[1] Chandra L. Tucker,[1] Ming Xiao,[1] Marianne C. Cilluffo,[4] Gordon L. Fain,[4] and James B. Hurley[1]

Departments of [1]Biochemistry and [2]Physiology and Biophysics, University of Washington, Seattle, Washington 98195, [3]Physiological Laboratory, University of Cambridge, Cambridge CB2 3EG, United Kingdom, and [4]Departments of Physiological Science and Ophthalmology, University of California Los Angeles, Los Angeles, California 90095-1606

Transducins couple visual pigments to cGMP hydrolysis, the only recognized phototransduction pathway in vertebrate photoreceptors. Here we describe a zebrafish mutant, *no optokinetic response f*^{w21} (*nof*), with a nonsense mutation in the gene encoding the α subunit of cone transducin. Retinal morphology and levels of phototransduction enzymes are normal in *nof* retinas, but cone transducin is undetectable. Dark current in *nof* cones is also normal, but it is insensitive to moderate intensity light. The *nof* cones do respond, however, to bright light. These responses are produced by a light-stimulated, but transducin-independent, release of Ca^{2+} into the cone cytoplasm. Thus, in addition to stimulating transducin, light also independently induces release of Ca^{2+} into the photoreceptor cytoplasm.

Key words: **genetic analysis of phototransduction; transducin; cone photoreceptor physiology; light adaptation; photoreceptor mutations; G-protein-mediated signal transduction**

Introduction

Phototransduction is the transformation of a light stimulus into an electrical response. Rod and cone photoactivated visual pigments stimulate transducin directly and catalytically, and the ensuing hydrolysis of cGMP closes cation channels in the photoreceptor outer segment plasma membrane (Ebrey and Koutalos, 2001). There are two amplification steps in this pathway, activation of transducin and hydrolysis of cGMP, that provide rods with enough sensitivity to detect single photons (Rieke and Baylor, 1998). Rod photoreceptors lacking transducin are unresponsive to light (Calvert et al., 2000).

In both rod and cone photoreceptors, a light-evoked decrease in the concentration of cytoplasmic free Ca^{2+} plays a central role in light adaptation (Matthews et al., 1988; Nakatani and Yau, 1988). In darkness, influx of Ca^{2+} through cGMP-gated channels is balanced by efflux via Na^+/K^+–Ca^{2+} exchange. Closure of channels by transducin-mediated phototransduction slows Ca^{2+} influx, whereas efflux continues. The resulting lowered cytoplasmic Ca^{2+} restores channels to their open state by stimulating guanylyl cyclase to synthesize more cGMP. This model for Ca^{2+} homeostasis and the role of Ca^{2+} in light adaptation is widely accepted, simple, and consistent with physiological and biochemical findings (Ebrey and Koutalos, 2001; Fain et al., 2001).

There are indications, however, that Ca^{2+} regulation in photoreceptors may be more complex than this model suggests. A prediction from the model is that light should have little effect on cytoplasmic Ca^{2+} when influx and efflux of Ca^{2+} are minimized by perfusion with solutions containing no Ca^{2+} or Na^+. However, recent studies show instead that light stimulates a rapid increase in intracellular Ca^{2+} under those conditions (Matthews and Fain, 2001, 2002). This suggests that there is a previously unrecognized mechanism for Ca^{2+} homeostasis in photoreceptors.

Photoreceptor types differ in several important aspects of their physiological function. Best appreciated is the difference between rods and cones. Cones are less sensitive to light than rods, but they respond over a much broader range of background intensities (Schnapf et al., 1990; Burkhardt, 1994). Cones also avoid saturation even in the presence of intense continuous illumination that bleaches >99% of their visual pigment (Burkhardt, 1994, 2001), a property not shared by rods. One approach to understanding the biochemical basis for physiological differences between photoreceptors is to evaluate the need for specific molecular components that are unique to particular photoreceptor types.

Here we investigate the role of transducin in cone phototransduction using a newly identified zebrafish mutant, *no optokinetic response f*^{w21} (*nof*). Because of a point mutation in the gene encoding the α subunit of cone transducin (Tcα), all four types of cones in this mutant have undetectable levels of Tcα protein. Not surprisingly, *nof* cones do not respond to light of dim to moderate intensity; however, the mutant cones do respond to bright light. We demonstrate that these responses are produced by a light-

Received Aug. 2, 2002; revised Oct. 21, 2002; accepted Oct. 24, 2002.

These studies were supported in part by Grants R01 EY06641 (J.B.H.), R01 EY012373 (S.E.B.), R01 EY01844 (G.L.F.), and R01EY011850 (F.R.) from the National Eye Institute, a grant from the Wellcome Trust (H.R.M.), and funds from the Howard Hughes Medical Institute. We thank Dan Possin for assistance with transmission electron microscopy, M. L. Woodruff and S. D. Anesi for assistance in calcium measurements, Laura Swaim for maintaining our zebrafish facility, A. P. Sampath for helpful discussions, and Drs. Peter Detwiler and Bertil Hille for comments on this manuscript. This paper is dedicated to the late Connie Lerea.

Correspondence should be addressed to Susan E. Brockerhoff, Department of Biochemistry, Box 357350, University of Washington, Seattle, WA 98195. E-mail: sbrocker@u.washington.edu.

C. H. Tucker's present address: Department of Genetics, Box 357360, University of Washington, Seattle, WA 98195.

Copyright © 2003 Society for Neuroscience 0270-6474/03/230470-11$15.00/0

stimulated, but transducin-independent, release of Ca^{2+} into the cone cytoplasm.

Materials and Methods

Mutant isolation and maintenance. The *nof* mutant was isolated in a three-generation screen of ethyl nitrosourea-mutagenized AB strain zebrafish using the optokinetic response (OKR) behavioral assay as described previously (Brockerhoff et al., 1998). Briefly, progeny from crosses between F2 siblings were partially immobilized in 6% methylcellulose (Sigma, St. Louis, MO), and their eye movements were analyzed in response to rotating illuminated stripes. In crosses between *nof* heterozygotes, 25% of the larvae showed no eye movements in white light. The stripe width used for the screen was 20°. Under normal conditions *nof* larvae do not survive to become adults. However, when we grew *nof* larvae with a 10× higher than normal concentration of paramecium, 50–100% of the mutant larvae would survive past 12 d post-fertilization (dpf). Between 12–20 dpf, *nof* mutants began to eat brine shrimp and then survived as well as wild-type (WT) larvae under the normal conditions of our fish facility. Fish that show a normal OKR (OKR+) include WT fish and fish heterozygous for the *nof* mutation. There were no obvious phenotypic differences in electrophysiology or histology between WT and heterozygous fish. For all experiments identifying and scoring polymorphisms, a hybrid strain between AB and WIK was used. WIK is a WT zebrafish strain that is polymorphic with the AB strain and is commonly used for mapping studies (Johnson and Zon, 1999). Because *nof* was generated in AB, this mutation segregated with AB markers. For single-cell recordings and Ca^{2+} measurements, animals used were between 2 and 3.5 months old.

Construction of adult zebrafish retina cDNA library. Retinas from pet store-purchased adult WT zebrafish were dissected away from the rest of the eye under a dissecting microscope and immediately placed on dry ice. Frozen retinas were then stored at −70°C before RNA isolation. Total RNA (273 μg) was isolated from 200 adult WT zebrafish retinas using RNAzol B (Tel-Test, Inc). Poly(A) Quik mRNA kit (Stratagene, La Jolla, CA) was used to isolate 20 μg mRNA. cDNA was synthesized using a Zap cDNA Gigapack III gold cloning kit (Stratagene) from 5 μg mRNA. The cDNA was then size selected using a Sephacryl S-500 column (Amersham Biosciences, Arlington Heights, IL). The average size of cDNA was between 500 and 3000 bp. The cDNA was then packaged into Lambda ZAP II vector (Stratagene). The primary library contained 9.5×10^5 plaque forming units (pfu). After amplification the titer of the library was 5.5×10^9 pfu/ml. All procedures were conducted following the manufacturer's instructions.

Histological analysis. Light and transmission electron microscopy (TEM) on mutant and sibling OKR+ larvae were done as described previously (Schmitt and Dowling, 1999). For TEM, 60–70 nm sections from two OKR+ and two *nof* larvae were analyzed.

In situ *hybridization. In situ* hybridization on whole-mount larvae was done as described previously (Brockerhoff et al., 1997). DNA encoding full-length Tcα, containing 52 bp of sequence upstream of the initiating ATG and 111 bp 3′ of the stop codon, was amplified from an adult zebrafish retinal cDNA library using taq DNA polymerase (Qiagen, Hilden, Germany) and ligated into TOPO2.1 cloning vector (Invitrogen, San Diego, CA). This clone was then digested with *Apa*I and *Bam*HI, and the resulting 1.2 Kb fragment was then subcloned into the pZErO-2 cloning vector (Invitrogen) that had also been digested with *Apa*I and *Bam*HI. Sense and antisense digoxigenin-labeled probes were synthesized using T7 and Sp6 polymerases, respectively. The approximate concentration of the probe used for hybridization was 1 ng/μl. *In situ* hybridization on 10 μm cryosections was done as described previously (Barthel and Raymond, 2000).

Cloning and mapping of zebrafish homologs of phototransduction genes. Degenerate primers and a nested PCR strategy were used to amplify 200–700 bp cDNA fragments from an adult zebrafish retina cDNA library with taq DNA polymerase (Qiagen) (see Table 1). Full-length clones were then obtained by either additional PCR or by screening the plated library. Primers used for mapping are listed in Table 1. cDNAs were mapped on either the LN 54 or the T 51 radiation hybrid panels as described (Geisler et al., 1999; Hukriede et al., 1999). All cDNA sequences have been submitted to the GenBank database. For sequence analysis, the full-length rod and cone transducin genes were amplified from the zebrafish retinal cDNA library using pfu DNA polymerase (Stratagene). The sequence of the pfu amplified clone has been submitted to GenBank (Table 1). Single-strand conformational polymorphism (SSCP) analysis was done as described (Foernzler and Beier, 1999).

Phosphodiesterase assay. Eyes from *nof* mutants and OKR+ zebrafish larvae were collected on ice and homogenized in 2× phosphodiesterase (PDE) buffer containing (in mM): 14 KCl, 10 NaCl, 6 $MgCl_2$, 2 DTT, 10 HEPES, pH 8.0, at a concentration of two eyes per 2.5 μl of buffer. Six microliters of homogenate were incubated for 5 min on ice with 2 μl of 1 mg/ml tosyl phenylalanyl chloromethylketone-treated trypsin (Sigma). Trypsin digestion was quenched with 2 μl of 12.5 mg/ml soybean trypsin inhibitor (Sigma). PDE was activated by the addition of 10 μl of substrate solution (1 mM ATP, 1 mM cGMP; specific activity ~50,000 cpm/μl in 1× PDE.) After a 5 min incubation at room temperature, samples were placed in a boiling water bath for 2–5 min. Two microliters of 5 mM cGMP/5 mM GMP were added to each sample, and the samples were then spun for 10 min at 14,000 rpm in a microfuge at 4°C. Six microliters of the reaction supernatant were spotted on a TLC plate (PEI cellulose; EM Science), and GMP and cGMP were separated using 0.2 M LiCl. Excised GMP was eluted in 1 ml of 2 M LiCl in a scintillation vial for 10 min with gentle rotation at room temperature. Six milliliters of scintillation fluid were added, and the samples were counted in a Beckman scintillation counter. All reactions were performed in duplicate, and the experiment was repeated twice.

Antibody production, Western blots, and immunocytochemistry. The peptide sequence n-MDRICKPDYLPT-c (aa 159–170) was used to generate rabbit polyclonal antibodies as described previously (Lerea et al., 1989). This sequence was chosen because the homologous region in mammalian Tcα has previously been shown to be antigenic (Lerea et al., 1986). This peptide sequence is unique to cone transducin and is not present in rod transducin. The antibody was affinity purified using a glutathione *S*-transferase fusion protein containing amino acid 141–180 of zebrafish Tcα. This fusion was also used to generate a rabbit polyclonal antibody that recognizes both rod and cone Tα. For Western blot analysis, affinity-purified anti-Tcα was diluted 1:50, anti-regulator of G-protein signaling (RGS) 9 (Cowan et al., 1998) was diluted 1:500, and anti-rod-cone Tα was diluted 1:2000. All immunoblotting was performed at least twice to confirm that all of the results shown are reproducible. Immunocytochemistry on 10 μm frozen sections was done as described previously (Brockerhoff et al., 1997). Cone Tα antibody was diluted 1:25, and antibody zpr1 was diluted 1:250. Secondary antibodies Cy2- and Cy3-conjugate (Jackson ImmunoResearch, West Grove, PA) were each diluted 1:200.

Single-cell recordings. Cone outer segment membrane currents were recorded from isolated cells with suction electrodes following established methods (Rieke and Baylor, 2000). Cells were superfused continuously with a Ringer's solution containing (in mM): 105 NaCl, 2 KCl, 30 $NaHCO_3$, 1.5 $CaCl_2$, 1.6 $MgCl_2$, 10 glucose, pH 7.4 when equilibrated with 5% CO_2/95% O_2. The solution filling the suction electrode was identical except that the $NaHCO_3$ was replaced with NaCl, and 3 mM HEPES was added. Light stimuli were delivered from light-emitting diodes (LEDs) with peak wavelengths of 470, 590, and 640 nm. Each recorded normal cone was identified as long wavelength (L), middle wavelength (M), short wavelength (S), or UV sensitive on the basis of the relative amplitude of their responses to flashes delivered from each of the three LEDs. We recorded from >30 L and M cones, each of which had a long and thin outer segment. The >15 recorded S and UV cones had much stouter outer segments. In recordings from *nof* cones, cells were identified as UV/S or L/M on the basis of their morphology.

Measurement of free Ca^{2+}. The free-calcium concentration was measured from the outer segments of normal and *nof* zebrafish cones as described previously for salamander photoreceptors (Sampath et al., 1998, 1999), modified by Matthews and Fain (2001). In brief, dissociated cones were incubated in darkness for 30 min with 10 μM fluo-4AM (Molecular Probes, Eugene, OR). The unincorporated dye was washed away, and the inner segments of the cones were drawn into a suction electrode so that the light response could be recorded, leaving the outer

Table 1. Genetic map position of candidate genes

Clone	LG	Position	LOD score (panel used)	Primers for mapping[a]	GenBank accession number
Transducin α (rod)	6	Between 54.8 and 57.3 cM from top	6 (T51)	MT2 /MT4	AY050499
Transducin α (cone)	8	Between 46.7 and 49.2 cM from top	13.2 (T51)	MT228 /MT229	AY050500
PDE γ (rod)	12	Between 49.9 and 51.1 cM from top	6.4 (T51)	MT5 /MT42	AY050506
Transducin γ (cone)	3	14.16 cR from fb34e06	14.4 (LN54)	MT269 /MT271	AY050507
GCAP-1	4	24.46 cR from Z9667	8.3 (LN54)	MT11 /MT12	AY050501
GCAP-2	23	39.96 cR from Z13363	7.4 (LN54)	MT13 /MT14	AY050502
RETGC-1	15	6.61 cR from Z8336	12.7 (LN54)	pKHD3F /pKHD3R	AY050503
RETGC-2	7	Between 53.5 and 59.1 cM from top	13.6 (T51)	pCAT6F /pCAT6R	AY050504
RETGC-3	5	18.03 cR from Z20915	9.6 (LN54)	MT47 /MT48	AY050505
GRK7	18	46.04 cR from Z10008	12.2 (LN54)	MT274 /MT275	AY050508
$GABA_b$ receptor	15	27.44 cR from Z9189	9.2 (LN54)	MT77 /MT79	AY050509

[a]Primer sequences available upon request. LOD, Log of the odds.

segments exposed to the bathing solution. A 9.2 μm spot from an argon ion laser (Model 60AT, American Laser Corporation, Salt Lake City, UT) tuned to 488 nm was focused onto the outer segments of the cones, and the emitted fluorescence was collected with a 505 nm dichroic mirror and a 510 nm emission filter (Omega Optical, Brattleboro, VT). The laser intensity was adjusted with neutral density filters to 1.7×10^{10} photons per square micrometer per second to keep dye bleaching to a minimum during the fluorescence measurement. Rapid solution changes from Ringer's to $0Ca^{2+}/0Na^{+}$ solution were made by laterally translating the microscope stage with a computer-controlled stepping motor (Matthews and Fain, 2001, 2002). The $0Ca^{2+}/0Na^{+}$ solution consisted of 111 mM choline chloride, 2.5 mM KCl, 2 mM EGTA, and 3 mM HEPES, adjusted to pH 7.7–7.8 with tetramethylammonium hydroxide.

Results

Identification of the *nof* mutant

The *nof* mutation was identified during an ongoing screen for recessive mutations that interfere with the vision-dependent OKR of zebrafish larvae (Brockerhoff et al., 1995, 1997, 1998). No OKR could be elicited from larvae homozygous for the *nof* mutation using white light. The *nof* mutation is inherited in a simple Mendelian manner as a recessive mutation. It has been maintained in our laboratory for several generations.

Mapping of candidate genes for vision mutants

In conjunction with our unbiased screen for vision mutants, we have also been mapping candidate genes, known genes that are likely to be needed for a normal optokinetic response. We generated an adult zebrafish retina cDNA library and cloned zebrafish homologs of several known phototransduction genes (Table 1). Our cDNA library was also provided to the Washington University EST project, and many additional expressed sequence tags (ESTs) have been sequenced and mapped by that group (http://zfish.wustl.edu/).

Mapping of *nof* and identification of the *nof* gene

The *nof* mutation was initially mapped by SSCP analysis using simple sequence length polymorphic markers selected for bulk segregant analysis (http://zebrafish.mgh.harvard.edu/cgi-bin/ssrmap/bulkseg_list.cgi). A linked polymorphism was identified with marker Z22270 indicating that *nof* is on linkage group 8 (LG8). Because Tcα is also on LG8 (Table 1), it was evaluated as a candidate gene. A polymorphism in Tcα was initially scored by SSCP analysis. No recombinants were found in the 50 *nof* mutants examined. The region surrounding the polymorphism, ~400 bp of Tcα genomic DNA (from cDNA bp 121–255) spanning intron 2, was then sequenced from *nof* and WT larvae. This sequence analysis identified a single nucleotide change that introduces a stop codon immediately before the second intron of the Tcα gene in the *nof* mutant. The full-length WT cDNA encodes a protein of 354 amino acids, and the mutation truncates the protein at position 52 (Fig. 1*A*). To confirm that the *nof* phenotype is caused by a Tcα mutation, we rescued it using a transgene that expresses normal full-length Tcα under control of a fragment of the zebrafish Tcα promoter. The OKR of ~14% of the *nof* mutants was restored by the presence of the transgene. The isolation and analysis of the promoter fragments will be described elsewhere (B. Kennedy, unpublished observations).

An alignment of the zebrafish and bovine Tcα amino acid sequences is shown in Figure 1*B*. Zebrafish Tcα is ~78% identical in amino acid sequence to its human, mouse, and bovine homologs. We also cloned the zebrafish rod transducin α subunit (Trα) and found it to be ~75% identical to zebrafish Tcα. This is similar to the identity between bovine rod and cone Tα (Lerea et al., 1986).

Tcα in WT zebrafish

To understand the effects of the Tcα mutation, we first characterized WT Tcα expression in zebrafish. Figure 2 shows the developmental time course of the appearance of Tcα mRNA. This pattern of expression mimics that seen for other genes expressed exclusively in cone photoreceptors such as cone opsins (Raymond et al., 1995). Tcα mRNA is first detectable at ~50 hr postfertilization (hpf) in the pineal (data not shown). By 2.5 dpf, Tcα mRNA also appears in a small patch in the ventral nasal retina (Fig. 2*A*). It then spreads within the ventral retina first in the

A

WT (41)AGESGKSTIVKQMK(54)...
nof ...AGESGKSTIVK--

B

```
      1                                                  50
zfish  MGSGASAEDKEMAKKSKELEKQLQEDADKEAKTVKLLLLGAGESGKSTIV
bovine MGSGASAEDKELAKRSKELEKKLQEDADKEAKTVKLLLLGAGESGKSTIV

     51                                                 100
zfish  KQMKILHQGGYTKEEQMEFRSIIFGNILQSALAIIRGMEMLSINFGSPSA
bovine KQMKIIHQDGYSPEECLEYKAIIYGNVLQSILAIIRAMPTLGIDYAEVSC

    101                                                 150
zfish  QEDSQKLQNLSDSIEEGTMPPELADVIKRLWKDAGVQASFDRAAEYQLND
bovine VDNGRQLNNLADSIEEGTMPPELVEVIRKLWKDGGVQACFDRAAEYQLND

    151                                                 200
zfish  SAGYYLNEMDRICKPDYLPTEQDVLRSRVKTTGIIEEQFGCKELHFRMFD
bovine SASYYLNQLDRITAPDYLPNEQDVLRSRVKTTGIIETKFSVKDLNFRMFD

    201                                                 250
zfish  VGGQRSERKKWIHCFEGVTCIIFCGALSAYDMVLVEDDEVNRMHESLHLF
bovine VGGQRSERKKWIHCFEGVTCIIFCAALSAYDMVLVEDDEVNRMHESLHLF

    251                                                 300
zfish  NSICNHRFFATTSIVLFLNKKDLFQEKIKKVHLSICFPDYDGPNTYEDAS
bovine NSICNHKFFAATSIVLFLNKKDLFEEKIKKVHLSICFPEYDGNNSYEDAG

    301                                                 350
 zfish NYIKTQFQDLNMKKGVKEIYSHMTCATDTKNVEIVFNAVTDIIIKENLKD
bovine NYIKSQFLDLNMRKDVKEIYSHMTCATDTQNVKFVFDAVTDIIIKENLKD

     351
 zfish CGLF-
bovine CGLF-
```

Figure 1. Identification of the Tcα mutation in *nof*. *A*, The *nof* mutation changes nucleotide 154 from a C to a T to introduce a stop codon (TAG) at amino acid position 52. *B*, Alignment of zebrafish Tcα with bovine Tcα. Nonconservative changes are indicated in *bold*.

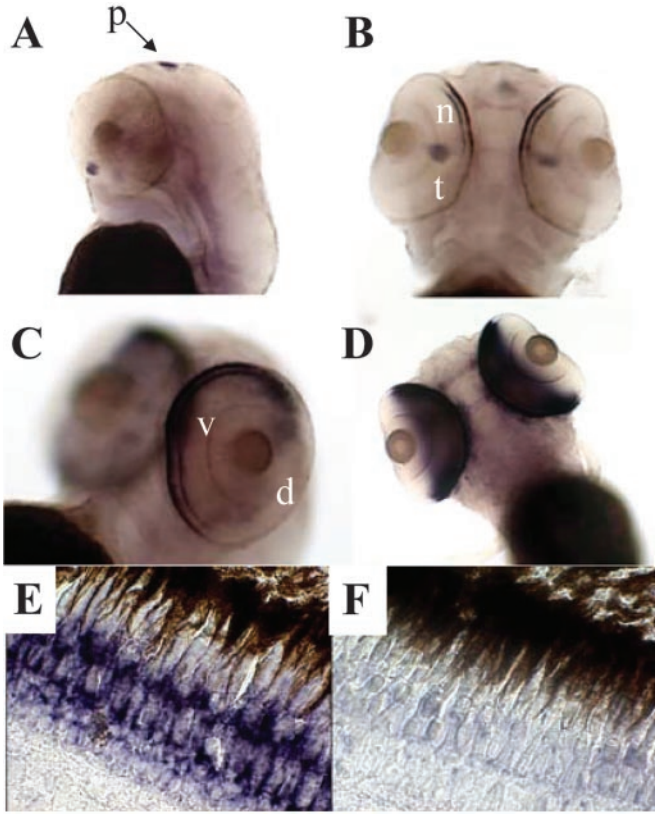

Figure 2. Tcα mRNA expression in larval and adult WT zebrafish. *A–E*, Antisense mRNA expression; *F*, sense control. Age of samples is between 52 and 56 hpf (*A*), between 70 and 74 hpf (*B*, *C*), between 79 nd 83 hpf (*D*), and adult (*E*, *F*). Refer to Results for a detailed description of the staining pattern. *p*, Pineal; *n*, nasal; *t*, temporal; *d*, dorsal; *v*, ventral; *y*, yolk. The dark staining of the yolk is nonspecific and is frequently seen with many other probes (Westerfield, 1995).

nasal direction and then in the temporal direction (Fig. 2*B*,*C*). By ~3.5 dpf, Tcα expression extends throughout both the dorsal and ventral retina (Fig. 2*D*).

To determine whether Tcα is expressed in all four types of cone photoreceptors—UV, short, middle, and long wavelength—we analyzed its expression using sections of WT adult zebrafish retinas. Distinct cone types are found at different layers in the adult zebrafish retina, so they can be identified on the basis of their depth in the retina (Raymond et al., 1993; Robinson et al., 1993). The results of *in situ* hybridization using Tcα probes on adult sections are shown in Figure 2*E*. All four cone types in the zebrafish retina express Tcα mRNA. The Tcα antisense probe labels the myoid regions of the short single (UV), long single (short wavelength), and double (middle and long wavelength) cones. Two rows of staining were observed. The proximal row is from short single cones, whereas the more distal row contains long single and double cones. In contrast, the sense riboprobe negative control did not label any cells in the retina (Fig. 2*F*). This result was confirmed by immunocytochemistry using a polyclonal antibody that specifically recognizes zebrafish Tcα. Zebrafish Tcα protein was found in the outer segments of all four types of cone photoreceptors but was not detected in rod photoreceptors (Fig. 3*C*).

Tcα in the *nof* mutant

Whole-mount *in situ* hybridization of 5 dpf larvae from a cross between *nof* heterozygotes revealed dramatically reduced levels of Tcα mRNA in ~25% of larvae as shown in Figure 3*A* ($n > 50$). Comparisons of retinal sections from mutants with OKR+ siblings revealed a profound reduction of mRNA levels at both 6 dpf and 2 months of age in the mutants (data not shown). This is consistent with reports that a premature stop codon often stimulates degradation of mRNA, a process referred to as nonsense-mediated mRNA decay (Frischmeyer and Dietz, 1999; Lykke-Andersen, 2001).

To characterize expression of Tcα protein we generated a polyclonal antibody to a peptide sequence unique to Tcα (see Materials and Methods). Figure 3*B* shows that the affinity-purified antibody recognizes a single polypeptide of the correct size to be zebrafish Tcα. With this antibody we were unable to detect any Tcα protein in *nof* using as much as 150× more *nof* eye homogenate than OKR+ homogenate (data not shown). We were also unable to detect Tcα in *nof* cone photoreceptors by immunocytochemical analyses (Fig. 3*C*). Because our antibody would not recognize the truncated form of cone transducin expressed from the *nof* gene, we cannot eliminate the possibility that this polypeptide is present in the mutant. However, the truncated protein would lack all the known functional domains of transducin except subdomains involved in Gβ and rhodopsin binding (Muradov and Artemyev, 2000; Slep et al., 2001). Such a short polypeptide could be unstable in the cell, and indeed, the *nof* mutation is recessive. Because we have not detected any phenotype in *nof* heterozygotes, it appears that if such a polypeptide is expressed, it does not influence phototransduction in cones.

Morphology

The functional consequence of the *nof* mutation is very specific. Figure 4*A* shows that the overall morphology and size of *nof* larvae at 5 dpf are normal. Nearly 100% of *nof* larvae develop

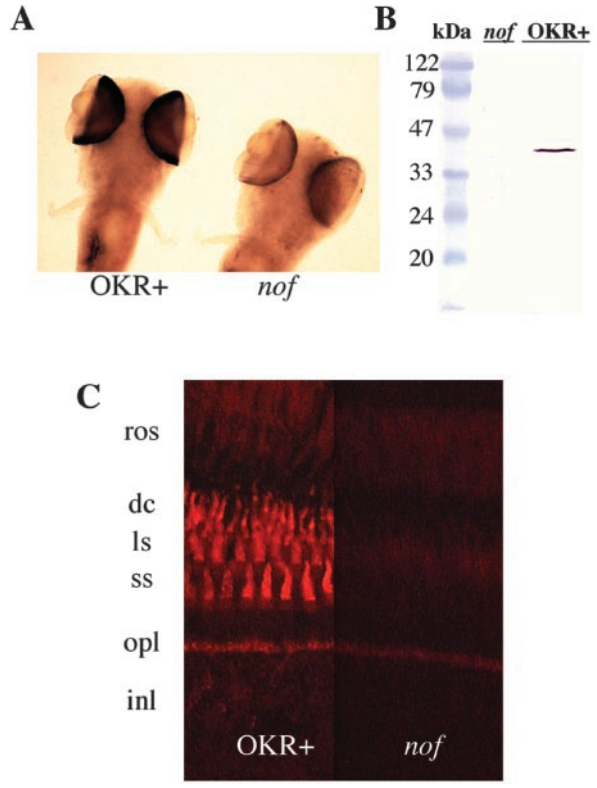

Figure 3. Tcα mRNA and protein expression in *nof* versus OKR+ zebrafish. *A*, *In situ* hybridization of *nof* and OKR+ larvae at 5 dpf shows that Tcα mRNA is dramatically reduced in the *nof* mutant. *B*, Western blot analysis of eye homogenates using affinity-purified Tcα polyclonal antibody. Tcα protein is undetectable in the *nof* mutant. *C*, Immunocytochemical analysis of OKR+ and *nof* retinas at 2 months using affinity-purified Tcα antibody. *ros*, Rod outer segments; *dc*, double cone; *ls*, long single cone; *ss*, short single cone; *opl*, outer plexiform layer; *inl*, inner nuclear layer.

normal swim bladders and swim actively starting at day 4 in a manner similar to OKR+ larvae. Externally, the eyes are of normal size and shape. Only one externally visible feature distinguishes *nof* from OKR+ larvae: the melanophores of homozygous *nof* larvae are slightly contracted in comparison to OKR+ larvae under ambient illumination. Because of this, *nof* larvae appear pale in comparison to their OKR+ siblings.

Figure 4*B* shows the retinal morphology of *nof* versus OKR+ zebrafish larvae at 5–6 dpf. The retina appears laminated, and all of the major cell types are present. There is no evidence of smaller or more darkly stained cells that would be signs of degeneration. Because Tcα protein is localized to cone outer segments (Fig. 3*C*), we analyzed the morphology of cone outer segments in *nof* and sibling OKR+ larvae using electron microscopy. No obvious morphological defects were detected in the cone outer segments at the EM level (Fig. 4*C*). The cone outer segment membranes were neatly organized in both the OKR+ and *nof* retinas. Thus, in contrast to many phototransduction mutants that cause photoreceptor degeneration or reduced outer segment length (for review, see Clarke et al., 2000), no cell death was apparent, and outer segments appeared normal in the *nof* mutant. Furthermore, no obvious signs of photoreceptor degeneration were detected by light microscopy in *nof* adults up to 1 year of age (data not shown), and immunocytochemical labeling with zpr1, an antibody that recognizes double cones, revealed a normal spacing of double cones in *nof* mutants as late as 2 months after fertilization (Fig. 5*A*). These results show that the *nof* retina is normal, and if any degeneration takes place it does so on a slow time scale.

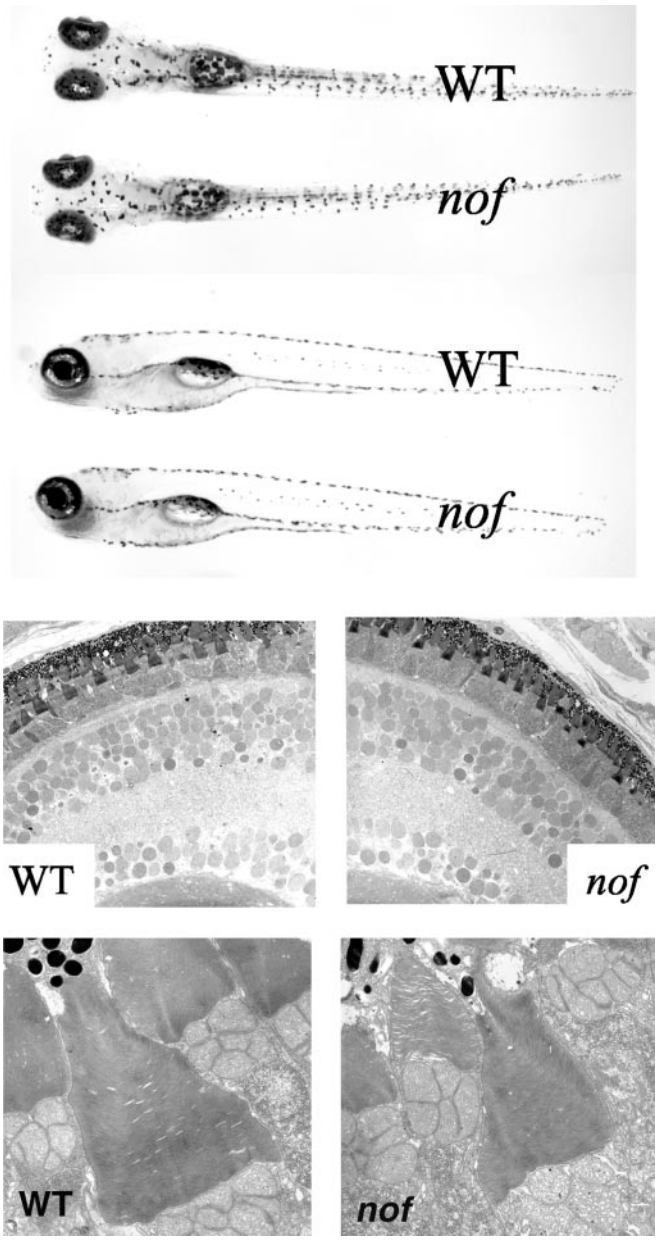

Figure 4. Normal morphology of the *nof* mutant. *A*, Dorsal (*top*) and lateral (*bottom*) view of *nof* and OKR+ larvae at 5 dpf. The *nof* mutant appears morphologically normal. Typical length of a 5 dpf is ~6 mm. *B*, *C*, The retina of *nof* appears normal. Light (*B*) and transmission electron microscopy (*C*) of *nof* and OKR+ retinas at 5–6 dpf are shown. Typical diameter of the eye at 5 dpf is ~300 μm. Scale bar (shown in *C*): 1 μm. *PRL*, Photoreceptor layer; *ONL*, outer nuclear layer; *IPL*, inner plexiform layer; *GCL*, ganglion cell layer; *L*, lens.

Probes for secondary effects of the *nof* mutation

We analyzed zebrafish *nof* mutants for secondary effects caused by the absence of Tcα by measuring the levels of phosphodiesterase (PDE), RGS9, and opsins, proteins that are expected to interact with Tcα. We also measured the levels of Trα in the *nof* mutant to determine whether it might be upregulated to compensate for the cone Tα mutation.

No antibody is yet available that recognizes cone PDE subunits in zebrafish. Instead we used activity measurements to estimate the levels of PDE subunits in OKR+ and *nof* cones. Because the majority of cGMP PDE activity in vertebrate retinal homogenates derives from photoreceptors, and because zebrafish retinas are functionally dominated by cones at 5 dpf

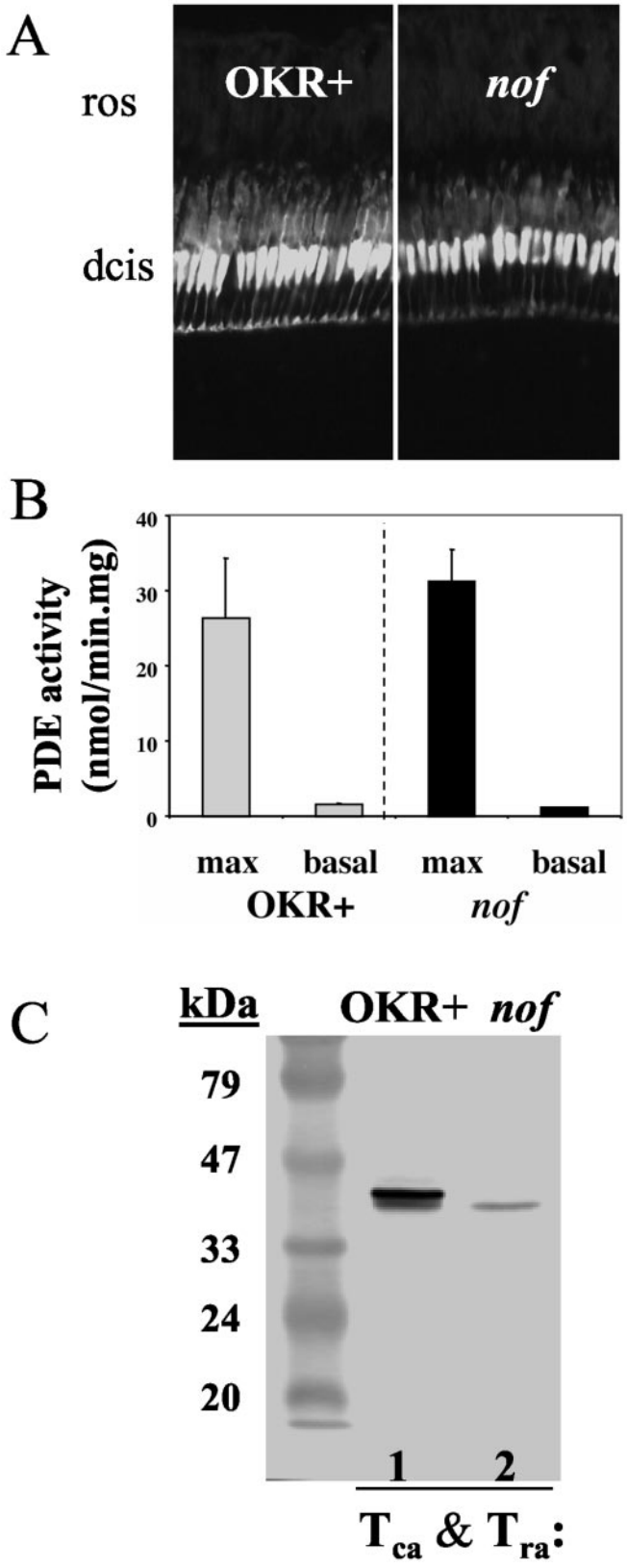

Figure 5. *A*, zpr1 staining of 2-month-old OKR+ and *nof* retinas. *ros*, Rod outer segments; *dcis*, double cone inner segments. *B*, PDE activity appears normal in the *nof* mutant. Measurements of basal and maximal PDE activity in homogenates of eyes from 5–7 dpf OKR+ and *nof* larvae are shown. *C*, Western blot analysis of homogenates of eyes from 5–7 dpf OKR+ and *nof* larvae. *Lanes 1* and *2* were labeled with an antibody that recognizes zebrafish rod and cone Tα subunits. Each *lane* corresponds to 5–10 larval eyes.

(Branchek, 1984; Van Epps et al., 2001), activity measurements should reflect the level of functional cone PDE. At 5 dpf, long-term dark adaptation of WT zebrafish does not affect the sensitivity of the visual response (Van Epps et al., 2001). The activity of photoreceptor PDE catalytic subunits in retinal homogenates is normally maintained in an inhibited state by a small γ subunit (Hamilton and Hurley, 1990) that is highly susceptible to degradation by trypsin (Hurley and Stryer, 1982). We measured the maximal PDE activity by treating *nof* and OKR+ larvae eye homogenates with trypsin to degrade the γ subunit specifically. There was no significant difference in either the basal (inhibited) or maximal (uninhibited) PDE activity between *nof* and OKR+ homogenates (Fig. 5*B*). The normal basal and maximal activity suggest that both the γ and α subunits of cone PDE are intact and present at normal or near-normal concentrations in the *nof* mutant. Additional evidence that in *nof* cones both PDE and guanylyl cyclase activities are normal is that *nof* cone photoreceptor dark currents are normal (see below).

To measure RGS9 we used the polyclonal antibody 4432 (kindly provided by T. Wensel, Baylor College of Medicine, Houston, TX) (Cowan et al., 1998). In zebrafish homogenates this antibody recognizes a protein of the correct size to be RGS9 that was equally abundant in OKR+ and *nof* larval homogenates (data not shown). Furthermore, we compared rhodopsin, UV cone, and long wavelength cone opsin protein levels at 4 and 14 months of age in OKR+ and *nof* fish (antibodies kindly provided by T. Vihtelic and D. Hyde, University of Notre Dame, South Bend, IN) (Vihtelic et al., 1999). We did not detect any difference in the levels of these opsin proteins between mutant and OKR+ fish (data not shown). These data show that loss of Tcα does not dramatically affect levels of specific proteins that it interacts with in the phototransduction cascade. These findings are consistent with the phenotype of mice in which the Trα subunit gene was inactivated (Calvert et al., 2000).

To measure Trα levels we used a polyclonal antibody that we generated against a fragment of zebrafish Tcα that includes regions of identity with Trα (see Materials and Methods). A doublet was detected on immunoblots of homogenates from OKR+ retinas (Fig. 5*C*, *lane 1*) corresponding to the expected sizes of Tcα and Trα. A fainter band with slower mobility was also detected, suggesting the presence of a small amount of a modified form of Tcα. Only the band with greatest mobility, corresponding to the slightly smaller mass of Trα, was detected in *nof* retina homogenates (Fig. 5*C*, *lane 2*). The intensity of the Trα signal was similar in OKR+ and *nof* homogenates.

Light responses and calcium measurements from single cones

To resolve whether *nof* cones respond to light, we recorded photoresponses directly from individual adult zebrafish cone photoreceptors. Both rods and cones in the adult retinas are suitable for suction electrode recordings using established methods (Rieke and Baylor, 2000). We also used the fluorescent indicator dye fluo-4 to measure light-induced changes in free-Ca^{2+} concentration with methods established previously for salamander photoreceptors (Sampath et al., 1998, 1999; Matthews and Fain, 2001).

Light responses from cones of adult homozygous *nof* mutants and from their OKR+ siblings are shown in Figure 6. Figure 6*A* shows average responses of a normal L cone to a series of 10 msec flashes of increasing intensity. Half-maximal responses were elicited by flashes producing 1000–2000 photoisomerizations. Figure 6*B* compares the flash responses of a normal cone to that of a *nof* cone to a flash 70× brighter. A similar lack of response was seen in >100 *nof* cones for flashes up to 200× brighter than those

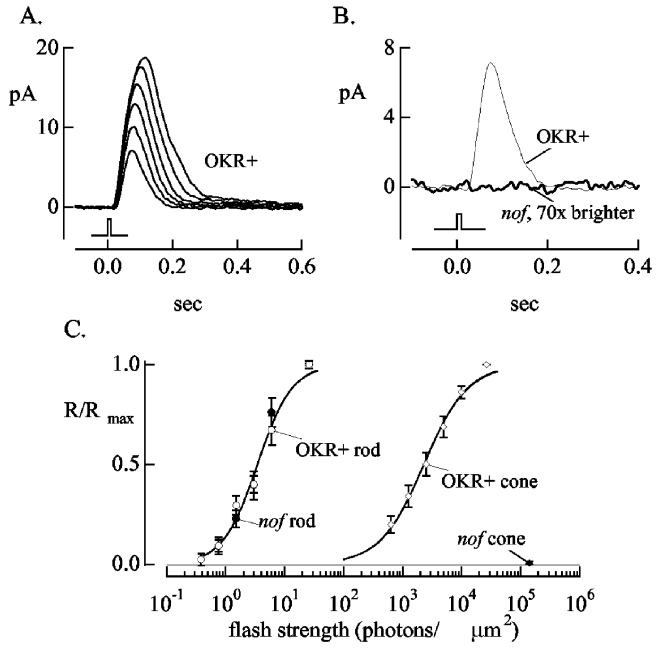

Figure 6. Photoreceptor responses of the *nof* mutant. *A*, Current recordings from an OKR+ L cone in response to 10 msec flashes of 590 nm light. The dimmest flash had a strength of 630 photons per square micrometer, and each successive flash was twice as bright. *B*, Response from a *nof* cone to a 10 msec flash of 44100 photons per square micrometer. For comparison the response of the OKR+ L cone from B to a flash 70× dimmer is shown. *C*, Comparison of the flash sensitivity of rods and cones from OKR+ (control) and *nof* fish. In contrast to cones, *nof* rods have normal sensitivity. Error bars are SE from recordings from 4 *nof* rods, 5 OKR+ rods, 73 *nof* cones, and 6 OKR+ cones. *Open circle*, OKR+ rod; *closed circle*, *nof* rod; *open diamond*, OKR+ cone; *closed diamond*, *nof* cone.

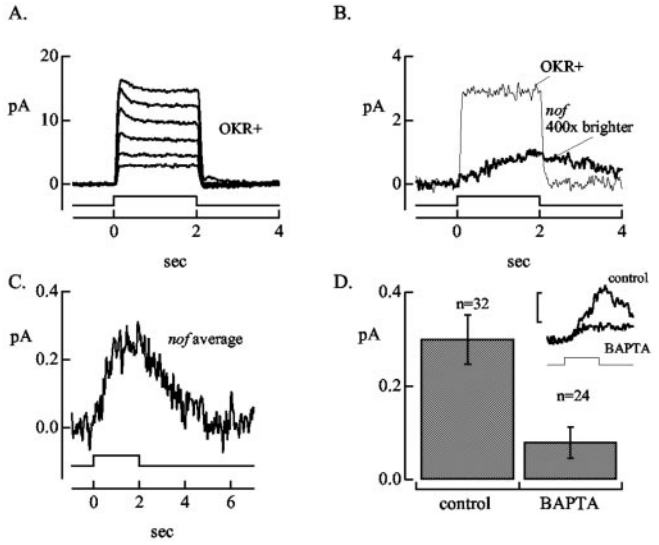

Figure 7. Small, Ca^{2+}-sensitive electrical responses are detected in *nof* cones during light steps. *A*, Shown is a family of step responses of 2 sec duration from an OKR+ L cone. The dimmest step had an intensity of 1575 photons per square micrometer per second, and each successive step was twice as bright. *B*, Comparison of step response from an OKR+ cone with the response of a *nof* cone to a light step 400× brighter. *C*, Average response of 26 *nof* cones to a 2 sec light step of intensity 1.3×10^7 photons per square micrometer per second. The averaged amplitude is significantly smaller than that obtained from the majority of individual cells because this average includes every *nof* cone from which responses to this step were measured. Some of the cells included in the average did not appear to respond. *D*, Comparison of the maximum amplitudes of *nof* cone responses with and without BAPTA loading. BAPTA dramatically reduced the response from *nof* cones. The *inset* shows the averaged responses from 2 sec stimuli. Calibration, 0.2 pA. The step intensity was 6.5×10^6 photons per square micrometer per second, and in all cases 590 nm light stimuli were used.

required to elicit half-maximal responses in normal cones. Figure 6*C* summarizes measurements of the flash sensitivity from 6 OKR+ cones and 73 *nof* cones. The *nof* cones that were analyzed included both L/M and S/UV cones. The lack of flash responses in *nof* cones indicated that their sensitivity was at least 1000 times less than that of their OKR+ siblings. Further evidence for the low sensitivity of *nof* cones came from measurements of their step responses (see below). Figure 6*C* also compares the sensitivity of rods from OKR+ and *nof* fish; the absence of Tcα had little or no effect on rod sensitivity, indicating that the *nof* mutation caused a specific defect in cone function.

The absence of Tcα could attenuate the light response directly, by reducing the efficiency of phototransduction, or indirectly, by altering the number of cGMP channels that are open in darkness. To distinguish between these two possibilities, we compared dark currents in OKR+ and *nof* cones by exposing their outer segments to 0.5 mM l-*cis*-diltiazem while recording membrane currents from the inner segments. This concentration of diltiazem reduced the dark current by 60–70% in OKR+ cones. The absolute magnitude of the current changes produced by diltiazem in six OKR+ and eight *nof* cones differed by <30% (data not shown). This indicates that OKR+ and *nof* cones maintain similar currents in darkness and that the differences we found in their light responses are caused by less efficient phototransduction in *nof*.

In addition to flash responses, we recorded responses to 2 sec light steps. Normal zebrafish cones responded rapidly to the onset and termination of a light step (Fig. 7*A*). Responses to dim steps reached a peak in 100–200 msec and maintained this level throughout the step. Responses to bright steps reached an initial peak and then sagged as light adaptation partially restored the current.

As expected from their insensitivity to light flashes, *nof* cones were 500–1000× less sensitive to steps than cones from OKR+ fish (32 *nof* cones, 12 normal cones). The *nof* cones, however, did generate small responses to steps that bleached a few percent of the cone visual pigment per second (Fig. 7*B*). Although the light needed to stimulate *nof* cones was bright, it was within the normal operational range for cone vision (Burkhardt, 1994). Step responses of individual *nof* cones ranged from near 0 pA to 1.5 pA. The cells that failed to respond included both L/M and S/UV cones; the fraction of cone cells that failed to respond was similar to that obtained with OKR+ fish. To determine the significance of these small responses, we averaged the response amplitude across all recorded cells, thus avoiding bias that would otherwise be introduced by selecting cells with apparent responses. The presence of a non-zero average response was highly significant (Fig. 7*D*) ($p < 0.0001$).

The kinetics of the step responses in the *nof* cones were also considerably slower than those of the normal cones (Fig. 7*B*). *nof* cone responses peaked in 1–1.5 sec compared with 0.1–0.2 sec for OKR+ cones; *nof* responses also recovered much more slowly than normal. The kinetics of the response in *nof* can be seen more clearly in Figure 7*C*, which shows the step response averaged from 26 *nof* cones plotted on a longer time scale to permit recovery of the response.

Because bright lights were required, we questioned whether the *nof* responses could be artifacts. The response clearly originated from the *nof* cones because the response was eliminated when all of the visual pigment in the cell was bleached (data not shown). Heating artifacts are unlikely, because photoreceptor dark current increases with temperature (Lamb, 1984), opposite to the response of *nof* to bright light.

We investigated whether the residual light responses of *nof* cones could be mediated by Ca^{2+}. Light normally causes a decline in cytoplasmic free-Ca^{2+} concentration in rod and cone outer segments because of suppression of Ca^{2+} influx and continued efflux by Na^+/K^+–Ca^{2+} exchange (Yau and Nakatani, 1985; Ratto et al., 1988; Gray-Keller and Detwiler, 1994; Sampath et al., 1998, 1999). Most of the Ca^{2+} decline is prevented when Na^+/K^+–Ca^{2+} exchange is inhibited by exposing the outer segment to $0Ca^{2+}/0Na^+$ solution (Matthews et al., 1988; Nakatani and Yau, 1988; Matthews and Fain, 2001). Recent experiments show, however, that exposure to $0Ca^{2+}/0Na^+$ solution not only greatly slows the light-stimulated Ca^{2+} decline but also enables a light-stimulated increase in free Ca^{2+} produced by release of Ca^{2+} from bound and/or sequestered stores (Matthews and Fain, 2001). Such a light-induced release of Ca^{2+} in *nof* cones might act on several targets, e.g., guanylyl cyclase or the cGMP-gated channels, to produce the observed changes in membrane current.

We tested directly for a light-induced change in Ca^{2+} concentration using the fluorometric indicator fluo-4. Laser illumination was used to evoke fluorescence from the indicator and to stimulate the cell. For cones from normal animals, exposure to laser light produced an initial small increase in fluorescence. Some part of this initial increase may reflect a process other than Ca^{2+} increase (Matthews and Fain, 2002; Woodruff et al., 2002). This was followed by a monotonic decline (Fig. 8*A*), likely produced by closure of cyclic nucleotide-gated channels and continued extrusion by Na^+/K^+–Ca^{2+} exchange. This decline is similar to that recorded previously from both rods and cones bathed in physiological saline (Yau and Nakatani, 1985; Ratto et al., 1988; Gray-Keller and Detwiler, 1994; Sampath et al., 1998, 1999). In *nof* cones (Fig. 8*B*), the fluorescence increase was much greater, because it was not superimposed on the rapid decline produced by complete cessation of Ca^{2+} influx. The increase was then followed by a small decline in fluorescence, probably from Na^+/K^+–Ca^{2+} exchange activity. This presumption is strengthened by the second trace in Figure 8*B*, showing the change in fluorescence in *nof* cones exposed to $0Ca^{2+}/0Na^+$ solution. Under this condition, exposure to the laser light produced an increase in fluorescence that, during the 2 sec duration of the laser exposure, continued to rise and showed no apparent decline like that recorded in Ringer's. The response of the mutant cones in $0Ca^{2+}/0Na^+$ solution resembles responses recorded in this solution for salamander rods (Matthews and Fain, 2001, 2002) and normal zebrafish cones (Fig. 8*A*) (Leung et al., 2002) and is likely to represent a sustained increase in free Ca^{2+}. These results show that light stimulates Ca^{2+} release even in the absence of transducin. The kinetics of Ca^{2+} release in the experiments shown in Figure 8 are not directly comparable with the current measurements shown in Figure 7 because they were stimulated with different sources of illumination.

If this Ca^{2+} increase is responsible for the light responses of *nof* cones, then the current reduction, recorded with suction electrodes, should be suppressed by chelating Ca^{2+} with BAPTA. We measured photocurrents from *nof* cones after bathing the cells in 50 μM BAPTA-AM for 15 min before electrical recording. Dark currents were not substantially altered in OKR+ cones after BAPTA loading, indicating that the treatment had little effect on resting Ca^{2+} levels in the outer segments (data not shown). BAPTA loading slowed and increased the amplitude of the responses of normal zebrafish cones (data not shown), effects similar to those observed previously in rods (Matthews et al., 1985; Korenbrot and Miller, 1986) and salamander cones (Sampath et al., 1999). Thus BAPTA effectively accumulates in zebrafish

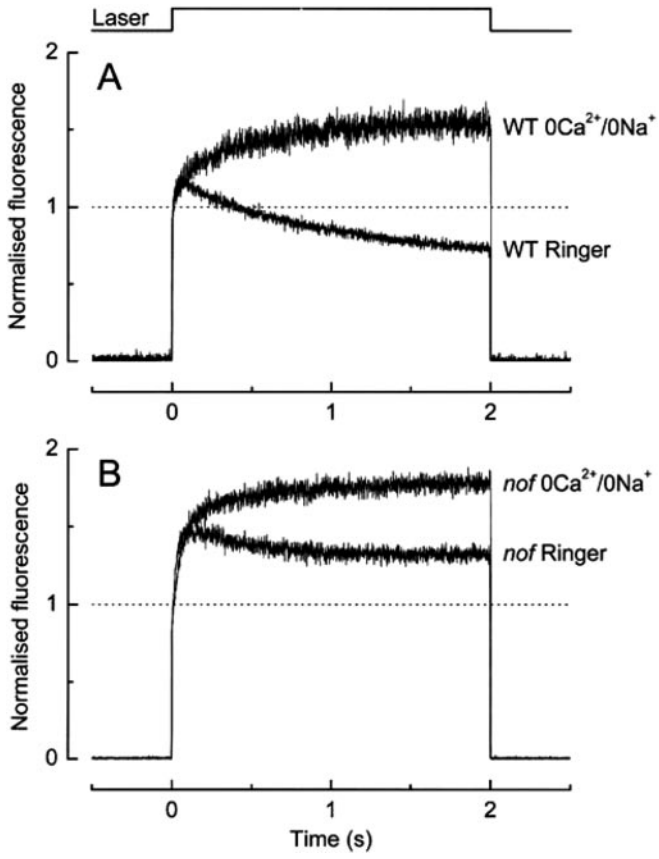

Figure 8. Change in free Ca^{2+} in cones from OKR+ and OKR− zebrafish cones. Fluorescence was recorded from zebrafish cones preloaded with fluo-4, a reporter of free Ca^{2+} concentration. Cones containing the dye were stimulated for 2 sec with intense laser light (see Materials and Methods). Traces are means from 13–25 cells, individually normalized to the mean value of the fluorescence recorded during the first 20 msec of laser illumination. *A*, Cones from OKR+ (*WT*) animals in Ringer's (*bottom trace*) produce a small increase in fluorescence followed by a decrease to a level substantially below the initial value. In $0Ca^{2+}/0Na^+$ solution (*top trace*), the fluorescence increases, but there is no subsequent decline. *B*, Stimulation of *nof* cones in Ringer's (*bottom trace*) produces a large increase in fluorescence followed by a slight decrease. Note that the final value of fluorescence remains substantially higher than the initial value, unlike in OKR+ cones. In $0Ca^{2+}/0Na^+$ solution (*top trace*), the fluorescence from *nof* cones increases with no subsequent decline, similar to $0Ca^{2+}/0Na^+$ responses from OKR+ cones.

cones and increases their Ca^{2+} buffering. Although BAPTA increased the sensitivity of OKR+ zebrafish cones, it reduced the amplitude of the light responses of *nof* cones approximately threefold. Figure 7*D* compares the amplitude of *nof* cone step responses with and without BAPTA. To ensure that the effect of BAPTA was not caused by chelation of zinc ions, we conducted a similar experiment using 10 μM *N*,*N*,*N*′,*N*′-terakis-(2pyridylmethyl)ethylenediamine (TPEN) (Arslan et al., 1985) instead of BAPTA. Unlike BAPTA, TPEN did not reduce the photoresponse obtained from *nof* cones (data not shown). The specific inhibitory effect of BAPTA on *nof* cones is consistent with the idea that *nof* photoresponses are mediated by a light-stimulated increase in Ca^{2+} that does not require transducin activation.

Discussion

This study uses a newly identified zebrafish mutant to address two questions. What role does Tcα play in light-stimulated suppression of the dark current, and what is the mechanism of Ca^{2+} release in cone photoreceptors? This study was possible because the *nof* mutation has very specific phenotypic consequences and

because zebrafish photoreceptors are amenable to single-cell recording methods.

One form of transducin is expressed in all cone types

A previous immunological study suggested that the same form of Tcα is expressed in all cone types in human retinas (Lerea et al., 1989). However, that study could not exclude the possibility that different transducins that are closely related and immunologically cross-reactive are expressed in different cones. The study described here shows that a single gene is used to express Tcα in all cones. This is consistent with the suggestion of the previous study and provides evidence that the gene from which Tcα is expressed is not responsible for differences in cone response properties. Also, unlike the fish *Sparus aurata*, which may contain only one transducin gene (Funkenstein and Jakowlew, 1997), zebrafish contain two transducin genes, one expressed in rods and the other expressed in cones.

Cone transducin is not required for photoreceptor formation or viability

Our study shows that the presence of Tcα is not essential for development of cones or for cone viability in young adult zebrafish. Electron microscopy, light microscopy, immunohistochemistry, and Western analysis all showed that the retina of *nof* fish develops normally and remains generally normal through adulthood. A further confirmation of the integrity of cone outer segments in older *nof* mutants came from our ability to perform single-cell suction recordings and fluorescence measurements from intact adult cone outer segments. Thus, if the absence of Tcα causes photoreceptor degeneration, then the degeneration must be slower and less severe than we can detect in the experiments that we have done with these animals.

Phototransduction is severely impaired but not absent in *nof*

A recent report described evidence that rod transducin is essential for phototransduction in mouse rods (Calvert et al., 2000). Likewise, we found that *nof* cones that lack Tcα fail to respond at low or moderate light levels. This confirms that Tcα is a requisite component of the phototransduction process under these illumination conditions.

Although moderate intensity stimuli do not evoke responses from *nof* cones, photoresponses can be elicited by bright light. When we stimulated *nof* cones with a step increase in light that bleached a few percent of their visual pigment per second, we detected a small, slow response that developed for ~1 sec after light onset. The kinetics of this response are qualitatively different from responses of normal cones, even for responses to very dim illumination. Because the dark currents of *nof* and normal cones differed by <30%, the small amplitude of the response reflects low sensitivity rather than a reduction in the number of channels open in darkness. These results show that phototransduction in *nof* cones, with its slow kinetics and small response amplitude, occurs via a mechanism that is much less efficient and qualitatively different from the major transducin-mediated phototransduction pathway.

Light stimulates Ca^{2+} release into the cytoplasm of *nof* cones

Phototransduction in cones is primarily mediated by changes in cGMP metabolism: as in rods, transducin stimulates hydrolysis of cGMP and closure of cation channels. Channel closure blocks Ca^{2+} entry, and the resulting depletion of intracellular Ca^{2+} provides negative feedback that reduces the amplitude and accelerates the kinetics of the photoresponse. Indeed, suppressing this feedback with BAPTA in normal zebrafish cones increases response amplitude and duration.

Light also has an additional effect on Ca^{2+} in rod and cone outer segments. It stimulates release of Ca^{2+} into the cytoplasm (Matthews and Fain, 2001, 2002; Leung et al., 2002). The light intensity used to stimulate Ca^{2+} release prompted an earlier suggestion that a mechanism less sensitive than normal phototransduction may be responsible for Ca^{2+} release (Matthews and Fain, 2001). The experiments described here demonstrate directly that transducin-mediated phototransduction is not required for light to stimulate Ca^{2+} release into the cytoplasm of zebrafish cones.

The best evidence for light-stimulated release of Ca^{2+} in *nof* cones is the comparison of fluo-4 signals in physiological versus $0Ca^{2+}/0Na^{+}$ solutions (Fig. 8*B*). Both rise rapidly immediately after onset of illumination. However, the signal in $0Ca^{2+}/0Na^{+}$ continues to rise, whereas in normal Ringer's it peaks early and then declines slowly. The rise in fluorescence most likely indicates release of Ca^{2+} into the cytoplasm; the slow decline in Ringer's indicates removal of Ca^{2+} by Na^{+}/K^{+}–Ca^{2+} exchange. This interpretation is consistent with the observation that the decline is faster when Ca^{2+} influx is slowed in normal zebrafish cones (Fig. 8*A*) and with the observation that exposure to $0Ca^{2+}/0Na^{+}$, which suppresses exchange, prevents the decline.

Relationship between Ca^{2+} release and the *nof* photoresponse

Increased cytoplasmic Ca^{2+} should inactivate cGMP-gated channels in cones by two mechanisms. First, Ca^{2+} reduces the affinity of the cone channel for cGMP (Hsu and Molday, 1993; Rebrik and Korenbrot, 1998), and second, Ca^{2+} inhibits synthesis of cGMP by photoreceptor membrane guanylyl cyclase (Koch and Stryer, 1988; Dizhoor et al., 1994; Palczewski et al., 1994; Dizhoor and Hurley, 1996).

The light-evoked increase in cytoplasmic Ca^{2+} could therefore explain the current suppression in *nof* cones. Consistent with this idea, the current suppression was reduced by Ca^{2+} buffering. This result is inconsistent with an explanation in which *nof* photoresponses are generated by very low, immunologically undetectable levels of cone or rod transducin, or even another G-protein. Those types of responses would be enhanced by Ca^{2+} buffering, as they are in normal cones, rather than reduced, as they are in *nof* cones. Electrical responses like those seen in *nof* cones have subsequently been recorded in mouse rods that lack Trα (M. L. Woodruff, H. R. Matthews, J. Lem, and G. L. Fain, unpublished observation). Taken altogether, these findings are most consistent with a mechanism in which activation of photopigments suppresses current using Ca^{2+} as a second messenger, altogether bypassing G-protein-mediated phosphodiesterase activation.

The kinetics of Ca^{2+} release in Figure 8*B* and the kinetics of current suppression in Figure 7*B* are not directly comparable because the responses were elicited by different stimuli. The decrease in fluorescence in Ringer's that occurs during the first 0.5 sec of intense illumination in Figure 8*B* may reflect depletion of the Ca^{2+} store in the presence of continuing exchanger activity. However, the release of Ca^{2+} by the less intense illumination used in the experiment shown in Figure 7*B* may be slower and more sustained. The Ca^{2+} store in that experiment may not have been depleted as rapidly or to the same extent as it was in the experiment shown in Figure 8*B*.

Significance of the *nof* photoresponse

The current responses recorded from *nof* cones were obtained with light intensities within the normal operational range for cone vision (Burkhardt, 1994, 2001). Could this type of phototransduction mechanism, uncovered by the *nof* mutation, be important for normal cone function? We consider two possibilities.

Sustaining a minimum Ca^{2+} level

On exposure to intense illumination, Ca^{2+} in rod and cone outer segments falls but fails to reach the level expected from the energetics of Na^+/K^+–Ca^{2+} exchange (Gray-Keller and Detwiler, 1994; Schnetkamp, 1995; Sampath et al., 1998, 1999). It is possible that low Ca^{2+} concentrations inhibit exchanger activity to prevent a further decline in Ca^{2+} (Schnetkamp and Szerencsei, 1993). However, the light-induced release of Ca^{2+} into the cytoplasm might also play a role in maintaining a plateau level of Ca^{2+} (Fain et al., 2001). Limiting depletion of intracellular free Ca^{2+} during exposure to bright light could serve several functions. One would be to keep the cell from fully light adapting on brief exposure to bright light (Calvert et al., 2002). Another possible reason to sustain a minimum Ca^{2+} concentration may be to prevent photoreceptor degeneration (Fain and Lisman, 1999).

Auxiliary phototransduction pathway

Cones avoid saturating even in the presence of background illumination that bleaches >99% of their visual pigment (Burkhardt, 1994, 2001). Under intense illumination, the rate of transducin activation in a cone may exceed the rate at which it can be inactivated. At that point, all transducins will be active, and further increases in illumination will cause no further physiological response through that pathway. The light-evoked increase of cytoplasmic Ca^{2+} and the electrical responses that we detected in *nof* cones may be indicators of an auxiliary phototransduction pathway that enables cones to respond under intense illumination. In intensely illuminated normal cones, an increase in cytoplasmic Ca^{2+} evoked by a strong stimulus would inhibit guanylyl cyclase, slow cGMP synthesis, and release cGMP from channels. With transducin saturated and phosphodiesterase hydrolyzing cGMP at its maximum velocity, there would be rapid depletion of cGMP, and channels would close. In principle these mechanisms would extend the operating range of cones. The current changes that we measured in dark-adapted *nof* mutant cones were small and slow, but light-evoked Ca^{2+} release ought to have more substantial effects on the biochemistry of light-adapted normal cones than on dark-adapted mutants. In normal cones, Ca^{2+} concentrations are low in the light-adapted state, and Ca^{2+} release would therefore cause large fractional changes in Ca^{2+} concentration and guanylyl cyclase activity. Furthermore, phosphodiesterase hydrolyzes cGMP at its maximum velocity under light-adapted conditions, so cGMP depletion in a light-adapted normal cone would be much faster than in dark-adapted *nof* cones.

Conclusion and perspective

Much effort has been devoted to understanding changes in free Ca^{2+} in photoreceptors because of the importance of Ca^{2+} as a messenger for adaptation. However, cytoplasmic free Ca^{2+} is only a small fraction of the total Ca^{2+} in photoreceptor outer segments. The concentration of free Ca^{2+} in the cytoplasm is ~0.5 μM, but total Ca^{2+} is at least 100× larger, ~50 μmol/l of tissue volume on the basis of Ca^{2+} buffering capacity measurements (Lagnado et al., 1992; Gray-Keller and Detwiler, 1994). In rods, the total Ca^{2+} concentration may be even greater than this (Schnetkamp, 1979; Fain and Schroder, 1985). The experiments with cones described here and elsewhere (Leung et al., 2002) together with previous experiments using rods (Matthews and Fain, 2001) indicate that movement of Ca^{2+} in photoreceptors between free and sequestered pools is affected by light. In our study using zebrafish *nof* mutants, we demonstrate experimentally that release of Ca^{2+} occurs independently of the transducin-mediated mechanism of phototransduction. The source of Ca^{2+} is unknown. In rod outer segments, some Ca^{2+} could be stored in the enclosed structures known as disks, but the absence of such structures in cones excludes them as a possible source of Ca^{2+}. It is more likely that Ca^{2+} is bound and released from sites in the cytoplasm or on the cytoplasmic face of the plasma membrane. Future biochemical and physiological studies may reveal the source of Ca^{2+}, the mechanism by which it is released, and the role of Ca^{2+} release in photoreceptor physiology.

References

Arslan P, Di Virgilio F, Beltrame M, Tsien RY, Pozzan T (1985) Cytosolic Ca^{2+} homeostasis in Ehrlich and Yoshida carcinomas. A new, membrane-permeant chelator of heavy metals reveals that these ascites tumor cell lines have normal cytosolic free Ca^{2}+. J Biol Chem 260:2719–2727.

Barthel LK, Raymond PA (2000) In situ hybridization studies of retinal neurons. Methods Enzymol 316:579–590.

Branchek T (1984) The development of photoreceptors in the zebrafish, *brachydanio rerio*. II. Function. J Comp Neurol 224:116–122.

Brockerhoff SE, Hurley JB, Janssen-Bienhold U, Neuhauss CF, Driever W, Dowling JE (1995) A behavioral screen for isolating zebrafish mutants with visual system defects. Proc Natl Acad Sci USA 92:10545–10549.

Brockerhoff SE, Hurley JB, Niemi GA, Dowling JE (1997) A new form of inherited red-blindness identified in zebrafish. J Neurosci 20:1–8.

Brockerhoff SE, Dowling JE, Hurley JB (1998) Zebrafish retinal mutants. Vision Res 38:1335–1339.

Burkhardt DA (1994) Light adaptation and photopigment bleaching in cone photoreceptors in situ in the retina of the turtle. J Neurosci 14:1091–1105.

Burkhardt DA (2001) Light adaptation and contrast in the outer retina. Prog Brain Res 131:407–418.

Calvert PD, Krasnoperova NV, Lyubarsky AL, Isayama T, Nicolo M, Kosaras B, Wong G, Gannon KS, Margolskee RF, Sidman RL, Pugh Jr EN, Makino CL, Lem J (2000) Phototransduction in transgenic mice after targeted deletion of the rod transducin alpha-subunit. Proc Natl Acad Sci USA 97:13913–13918.

Calvert PD, Govardovskii VI, Arshavsky VY, Makino CL (2002) Two temporal phases of light adaptation in retinal rods. J Gen Physiol 119:129–146.

Clarke G, Heon E, McInnes RR (2000) Recent advances in the molecular basis of inherited photoreceptor degeneration. Clin Genet 57:313–329.

Cowan CW, Fariss RN, Sokal I, Palczewski K, Wensel TG (1998) High expression levels in cones of RGS9, the predominant GTPase accelerating protein of rods. Proc Natl Acad Sci USA 95:5351–5356.

Dizhoor AM, Hurley JB (1996) Inactivation of EF-hands makes GCAP-2 (p24) a constitutive activator of photoreceptor guanylyl cyclase by preventing a Ca^{2+}-induced "activator-to-inhibitor" transition. J Biol Chem 271:19346–19350.

Dizhoor AM, Lowe DG, Olshevskaya EV, Laura RP, Hurley JB (1994) The human photoreceptor membrane guanylyl cyclase, RetGC, is present in outer segments and is regulated by calcium and a soluble activator. Neuron 12:1345–1352.

Ebrey T, Koutalos Y (2001) Vertebrate photoreceptors. Prog Retin Eye Res 20:49–94.

Fain GL, Lisman JE (1999) Light, Ca^{2+}, and photoreceptor death: new evidence for the equivalent-light hypothesis from arrestin knockout mice. Invest Ophthalmol Vis Sci 40:2770–2772.

Fain GL, Schroder WH (1985) Calcium content and calcium exchange in dark-adapted toad rods. J Physiol (Lond) 368:641–665.

Fain GL, Matthews HR, Cornwall MC, Koutalos Y (2001) Adaptation in vertebrate photoreceptors. Physiol Rev 81:117–151.

Foernzler D, Beier DR (1999) Gene mapping in zebrafish using single-

strand conformation polymorphism analysis. Methods Cell Biol 60:185–193.
Frischmeyer PA, Dietz HC (1999) Nonsense-mediated mRNA decay in health and disease. Hum Mol Genet 8:1893–1900.
Funkenstein B, Jakowlew SB (1997) Piscine (*Sparus aurata*) alpha subunit of the G-protein transducin is homologous to mammalian cone and rod transducin. Vision Res 37:2487–2493.
Geisler R, Rauch GJ, Baier H, van Bebber F, Brobeta L, Dekens MP, Finger K, Fricke C, Gates MA, Geiger H, Geiger-Rudolph S, Gilmour D, Glaser S, Gnugge L, Habeck H, Hingst K, Holley S, Keenan J, Kirn A, Knaut H, et al. (1999) A radiation hybrid map of the zebrafish genome. Nat Genet 23: 86–89.
Gray-Keller MP, Detwiler PB (1994) The calcium feedback signal in the phototransduction cascade of vertebrate rods. Neuron 13:849–861.
Hamilton SE, Hurley JB (1990) A phosphodiesterase inhibitor specific to a subset of bovine retinal cones. J Biol Chem 265:11259–11264.
Hsu YT, Molday RS (1993) Modulation of the cGMP-gated channel of rod photoreceptor cells by calmodulin. Nature 361:76–79.
Hukriede NA, Joly L, Tsang M, Miles J, Tellis P, Epstein JA, Barbazuk WB, Li FN, Paw B, Postlethwait JH, Hudson TJ, Zon LI, McPherson JD, Chevrette M, Dawid IB, Johnson SL, Ekker M (1999) Radiation hybrid mapping of the zebrafish genome. Proc Natl Acad Sci USA 96:9745–9750.
Hurley JB, Stryer L (1982) Purification and characterization of the gamma regulatory subunit of the cyclic GMP phosphodiesterase from retinal rod outer segments. J Biol Chem 257:11094–11099.
Johnson SL, Zon LI (1999) Genetic backgrounds and some standard stocks and strains used in zebrafish developmental biology and genetics. Methods Cell Biol 60:357–359.
Koch KW, Stryer L (1988) Highly cooperative feedback control of retinal rod guanylate cyclase by calcium ions. Nature 334:64–66.
Korenbrot JI, Miller DL (1986) Calcium ions act as modulators of intracellular information flow in retinal rod phototransduction. Neurosci Res [Suppl] 4:S11–34.
Lagnado L, Cervetto L, McNaughton PA (1992) Calcium homeostasis in the outer segments of retinal rods from the tiger salamander. J Physiol (Lond) 455:111–142.
Lamb TD (1984) Effects of temperature changes on toad rod photocurrents. J Physiol (Lond) 346:557–578.
Lerea CL, Somers DE, Hurley JB, Klock IB, Bunt-Milam AH (1986) Identification of specific transducin alpha subunits in retinal rod and cone photoreceptors. Science 234:77–80.
Lerea CL, Bunt-Milam AH, Hurley JB (1989) Alpha transducin is present in blue-, green-, and red-sensitive cone photoreceptors in the human retina. Neuron 3:367–376.
Leung YT, Fain GL, Matthews HR (2002) Measurement of Ca^{2+} during the flash response without pigment bleaching in isolated UV-sensitive zebrafish cones. J Physiol Proc 539:142–143.
Lykke-Andersen J (2001) mRNA quality control: marking the message for life or death. Curr Biol 11:R88–91.
Matthews HR, Fain GL (2001) A light-dependent increase in free Ca^{2+} concentration in the salamander rod outer segment. J Physiol (Lond) 532:305–321.
Matthews HR, Fain GL (2002) Time course and magnitude of the calcium release induced by bright light in salamander rods. J Physiol (Lond) 542: 829–841.
Matthews HR, Torre V, Lamb TD (1985) Effects on the photoresponse of calcium buffers and cyclic GMP incorporated into the cytoplasm of retinal rods. Nature 313:582–585.
Matthews HR, Murphy RL, Fain GL, Lamb TD (1988) Photoreceptor light adaptation is mediated by cytoplasmic calcium concentration. Nature 334:67–69.
Muradov KG, Artemyev NO (2000) Coupling between the N- and C-terminal domains influences transducin-alpha intrinsic GDP/GTP exchange. Biochemistry 39:3937–3942.
Nakatani K, Yau KW (1988) Calcium and light adaptation in retinal rods and cones. Nature 334:69–71.
Palczewski K, Subbaraya I, Gorczyca WA, Helekar BS, Ruiz CC, Ohguro H, Huang J, Zhao X, Crabb JW, Johnson RS (1994) Molecular cloning and characterization of retinal photoreceptor guanylyl cyclase-activating protein. Neuron 13:395–404.
Ratto GM, Payne R, Owen WG, Tsien RY (1988) The concentration of cytosolic free calcium in vertebrate rod outer segments measured with fura-2. J Neurosci 8:3240–3246.
Raymond PA, Barthel LK, Rounsifer ME, Sullivan SA, Knight JK (1993) Expression of rod and cone visual pigments in goldfish and zebrafish: a rhodopsin-like gene is expressed in cones. Neuron 10:1161–1174.
Raymond PA, Barthel LK, Curran GA (1995) Developmental patterning of rod and cone photoreceptors in embryonic zebrafish. J Comp Neurol 359:537–550.
Rebrik TI, Korenbrot JI (1998) In intact cone photoreceptors, a Ca^{2+}-dependent, diffusible factor modulates the cGMP-gated ion channels differently than in rods. J Gen Physiol 112:537–548.
Rieke F, Baylor DA (1998) Origin of reproducibility in the responses of retinal rods to single photons. Biophys J 75:1836–1857.
Rieke F, Baylor DA (2000) Origin and functional impact of dark noise in retinal cones. Neuron 26:181–186.
Robinson J, Schmitt EA, Harosi FI, Reece RJ, Dowling JE (1993) Zebrafish ultraviolet visual pigment: absorption spectrum, sequence, and localization. Proc Natl Acad Sci USA 90:6009–6012.
Sampath AP, Matthews HR, Cornwall MC, Fain GL (1998) Bleached pigment produces a maintained decrease in outer segment Ca^{2+} in salamander rods. J Gen Physiol 111:53–64.
Sampath AP, Matthews HR, Cornwall MC, Bandarchi J, Fain GL (1999) Light-dependent changes in outer segment free-Ca^{2+} concentration in salamander cone photoreceptors. J Gen Physiol 113:267–277.
Schmitt EA, Dowling JE (1999) Early retinal development in the zebrafish, *Danio rerio*: light and electron microscopic analyses. J Comp Neurol 404:515–536.
Schnapf JL, Nunn BJ, Meister M, Baylor DA (1990) Visual transduction in cones of the monkey *Macaca fascicularis*. J Physiol (Lond) 427:681–713.
Schnetkamp PP (1979) Calcium translocation and storage of isolated intact cattle rod outer segments in darkness. Biochim Biophys Acta 554:441–459.
Schnetkamp PP (1995) How does the retinal rod Na-Ca+K exchanger regulate cytosolic free Ca^{2+}? J Biol Chem 270:13231–13239.
Schnetkamp PP, Szerencsei RT (1993) Intracellular Ca^{2+} sequestration and release in intact bovine retinal rod outer segments. Role in inactivation of Na-Ca+K exchange. J Biol Chem 268:12449–12457.
Slep KC, Kercher MA, He W, Cowan CW, Wensel TG, Sigler PB (2001) Structural determinants for regulation of phosphodiesterase by a G protein at 2.0 A. Nature 409:1071–1077.
Van Epps HA, Yim CM, Hurley JB, Brockerhoff SE (2001) Investigations of photoreceptor synaptic transmission and light adaptation in the zebrafish visual mutant nrc. Invest Ophthalmol Vis Sci 42:868–874.
Vihtelic TS, Doro CJ, Hyde DR (1999) Cloning and characterization of six zebrafish photoreceptor opsin cDNAs and immunolocalization of their corresponding proteins. Vis Neurosci 16:571–585.
Westerfield M (1995) . The zebrafish book: a guide for the laboratory use of zebrafish (*Brachydanio rerio*). Eugene, OR: University of Oregon.
Woodruff ML, Sampath AP, Matthews HR, Krasnoperova NV, Lem J, Fain GL (2002) Measurement of cytoplasmic calcium concentration in the rods of wild-type and transducin knock-out mice. J Physiol (Lond) 542:843–854.
Yau KW, Nakatani K (1985) Light-induced reduction of cytoplasmic free calcium in retinal rod outer segment. Nature 313:579–582.